Photocatalysts

DOI: 10.1002/anie.201302525

Self-Organized Arrays of Single-Metal Catalyst Particles in TiO_2 Cavities: A Highly Efficient Photocatalytic System**

*Jeong Eun Yoo, Kiyoung Lee, Marco Altomare, Elena Selli, and Patrik Schmuki**

Photocatalytic reactions are based on the interaction of light with a semiconductor that is immersed in a suitable reaction environment.[1] The light, if of sufficient energy ($> E_g$), creates electrons and holes that then can be captured from the semiconductor surface by redox states in the environment, namely a liquid or gas. Hole transfer from the valence band to the environment may be exploited for oxidation reactions, and electron transfer from the conduction band may be used for reduction reactions. Essentially, this simple principle has an extremely large potential for applications.[2–8] Currently, photocatalytic features are widely explored to tackle several contemporary global challenges, including pollutant degradation (hydrocarbons, CO_2, NO_x),[9,10] formation of innovative self-cleaning systems,[11] or to create hydrogen from solar energy, which is currently at the forefront of interest.[2,12] In the most straightforward approach, a photocatalyst is simply immersed into suitable source of a renewable substance, such as water or ethanol, and both the oxidation and reduction reaction take place simultaneously on the illuminated semiconductor surface. In practice, the charge transfer from the conduction or valence band to the environment may be strongly kinetically hindered and the semiconductor needs to be decorated by suitable charge-transfer catalysts, such as noble metal particles, to reach reasonable conversion efficiencies.

By far the most used semiconductive material for UV photocatalysis is TiO_2, which has a number of beneficial features but typically shows a very sluggish kinetics, if it is used, for example, to form H_2 from H_2O or EtOH by excited conduction-band electrons. Therefore, TiO_2 is frequently used in combination with classic catalysts (Pt, Au) to achieve a more efficient H_2O or EtOH reduction to H_2.[13] For EtOH oxidation, CO poisoning of Pt takes place and thus gold is mostly used as a co-catalyst. Classic Au@TiO_2 catalysts are based either on TiO_2 nanoparticles or a compact, flat TiO_2 surface onto which Au particles are deposited using mainly electroless deposition approaches.

This typically leads to a relatively inhomogeneous deposition of particles in terms of size and spacing. The process provides a comparably low amount of control to optimize the geometry of semiconductor, as well as particle location, size, and agglomerate distribution. It can therefore be easily envisaged that these effects lead to suboptimum efficiency and a certain lack of control over the process.

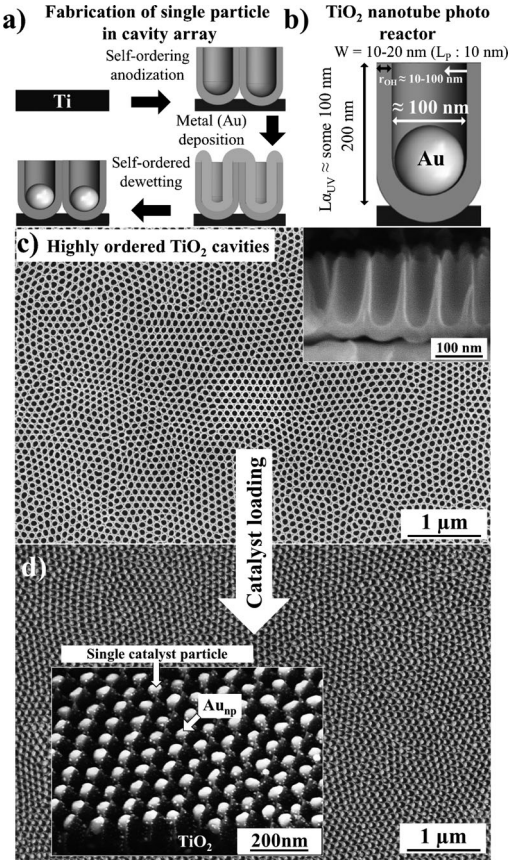

Figure 1. a) Fabrication of an array of single catalytic particles, embedded in ideal individual TiO_2 nanocavities by self-organizing anodic TiO_2 nanotube-stump formation, catalyst metal film deposition, and self-ordered dewetting of the metal film. b) The photocatalytic reactor in view of UV absorption ($L\alpha_{UV}$ vs. tube length), hole diffusion length (L_p vs. wall thickness), and range of photocatalytically generated radicals (rOH* vs. tube inner diameter). c) SEM images of a highly ordered TiO_2 cavity array (individual cavity length ca. 200 nm, top width ca. 80 nm, wall thickness ca. 15 nm) produced on Ti by self-organizing anodization (top and side view). d) Total filling with exactly one catalyst particle per cavity (details on the synthesis are given in the Supporting Information).

[*] J. E. Yoo, K. Lee, M. Altomare, Prof. Dr. P. Schmuki
Department Werkstoffwissenschaften
Universität Erlangen-Nürnberg
Martensstrasse 7, 91058 Erlangen (Germany)
E-mail: Schmuki@ww.uni-erlangen.de
Prof. Dr. P. Schmuki
Department of Chemistry, King Abdulaziz University
Jeddah (Saudi Arabia)
M. Altomare, Prof. Dr. E. Selli
Dipartimento di Chimica, Universitá degli Studi di Milano
via C. Golgi 19, 20133 Milano (Italy)

[**] The authors would like to acknowledge the DFG and DFG cluster of excellence EAM for financial support and H. Hildebrand for valuable technical help.

Supporting information for this article is available on the WWW under http://dx.doi.org/10.1002/anie.201302525.

The present work introduces an entirely novel highly defined $Au_{np}@TiO_2$ platform as outlined in Figure 1, and we demonstrate its beneficial use for the photocatalytic oxidation of EtOH to H_2. The construction of the highly ordered photocatalytic surface of Figure 1 relies on a synergetic overlay of two self-organizing concepts. In a first step, we form a surface consisting of self-organized TiO_2 nanocavities: these are not only a very effective semiconductor geometry for photocatalysis but also provide the ideal hexagonally patterned surface that is an absolute prerequisite for a highly controlled self-ordering in the subsequent metal dewetting step.

The TiO_2 nanotube stumps are formed in principle by classic self-ordering anodization. Nevertheless, we found that the degree of ordering of many previous nanotube growth methods is not sufficient to achieve ideal dewetting. To optimize ordering, we adopted a concept for maximum self-organization outlined for porous alumina; that is, that high rate of oxide growth combined with a high oxide dissolution rate leads to maximal ordering.[14–16]

For TiO_2, we developed a self-ordering approach to anodically grow TiO_2 nanotubes in a hot H_3PO_4/HF solution, which provides the desired high-rate oxidation/dissolution equilibrium and indeed leads to an unprecedented degree of ordering (see the Supporting Information for details). This anodization approach also allows tube growth to be tailored to the very short tube length; that is, in the shape of cavities that are needed for ordering in the subsequent metal-dewetting process. It is also noteworthy that the resulting TiO_2 cavity is ideal for UV-based photocatalytic reactions. It is around 200 nm deep and 80 nm in diameter, and thus provides a highly optimized photocatalytic reaction-vessel geometry regarding the absorption length of UV (some 100 nm cavity length), the range of generated radicals from the TiO_2 surface into the environment (for example, OH* of 10–100 nm) and a solid-state diffusion length for holes in the range of the TiO_2 cavity wall thickness. In other words, the vessel confines the entire reactive scenario essentially into the inside of a single nanocavity.

To create the Au loading of the cavities, we thermally dewetted thin Au layers that were sputter-deposited onto the nanocavity layers (see the Supporting Information for experimental details). As such, dewetting of a thin solid metal film on a substrate is a common method for preparing metallic particles on large areas.[16–20] If carried out on a flat surface, the dewetting process results in metal islands with broad distributions of size and spacing, as in this case dewetting by film rupture must take place at random defects (Supporting Information, Figure S2). However, by using a periodic substrate surface topography (that is, providing defined rupture initiation sites), it becomes possible to control the dewetting process. Such approaches are emerging in the field of semiconductor technology using for example lithographically structured Si/SiO_2 surfaces.[21] For optimum self-organization, not only the spacing and height of the cavity need to be considered and aligned to the thickness of the sputtered metal film, but even more importantly, the degree of self-organizing needs to be extremely high, otherwise self-ordered dewetting will occur in a massively imperfect fashion (Supporting Information, Figure S3). In this context, it is also noteworthy that the annealing atmosphere was found to be of a significant influence (Supporting Information, Figure S4).

For the structures in Figure 1d, we deposited a 20 nm thick Au film uniformly on the surface (Figure 1c) and dewetted the film by a thermal treatment at 450 °C for 30 min in air. Evidently this treatment leads to a highly ordered TiO_2 nanocavity array filled with exactly one Au catalyst particle per cavity (Figure 1d). This filling takes place over large surface areas (cm^2) with a success rate of more than 99.9 %.

Figure 2 illustrates several aspects of the array formation as well as SEM, XRD, and XPS characterization after individual formation steps. After several attempts, we found it most useful to characterize the regularity of the TiO_2 cavities by FFT conversion of the image (Figure 2a,b;

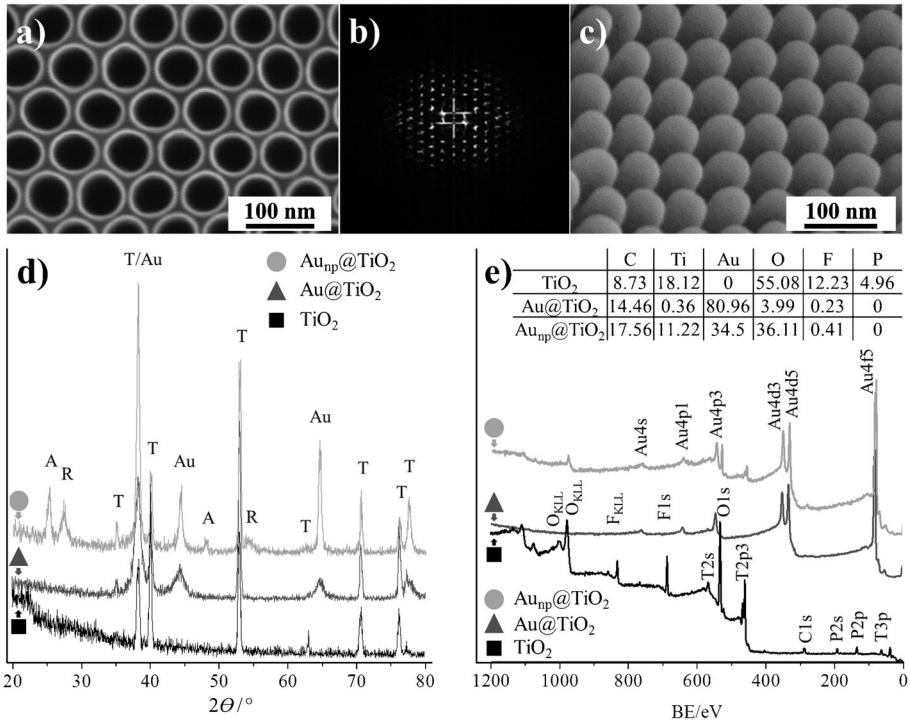

Figure 2. a) SEM image of a highly ordered TiO_2 cavity array fabricated on a Ti metallic substrate by anodization in hot 3 M HF/H_3PO_4 electrolyte (top view). b) FFT conversion of (a). c) Metal replica by sputtering the ideal filling of the TiO_2 cavities. d) X-ray diffraction patterns and e) X-ray photoelectron spectroscopy for as-formed TiO_2, Au-sputtered TiO_2, and dewetted Au nanoparticles on the TiO_2 substrate. T = Ti, A = anatase, R = rutile, Au = gold.

a comparison of the approach with various self-organized nanotubes formed by other methods is shown in the Supporting Information). After the deposition of a thin metal layer by sputtering, the ideal filling of the cavity can be observed if the Ti/TiO_2 substrate is selectively etched off in HF (Figure 2c), leaving a highly regular metal replica behind.

XRD and XPS (Figure 2d,e) demonstrate that after formation, the cavities consist of amorphous TiO_2 with typical P and F uptake. XPS high-resolution peaks are given in the Supporting Information, Figure S5. After Au deposition, only Au is apparent in the top-view XPS, indicating the presence of a completely closed Au layer on the TiO_2 cavities. After thermal dewetting, the top-view XPS shows that the TiO_2 substrate becomes visible again (owing to the exposure of dewetted substrate). From XRD after dewetting, it is clear that the treatment of 450 °C leads, as desired, not only to the isolated Au particles but at the same time to a conversion of the amorphous TiO_2 to fully crystalline TiO_2 cavities consisting of a mixture of anatase and rutile.

To demonstrate the straightforward use of such structures in a highly relevant photocatalytic application, we used Au_{np}@TiO_2 nanocavity arrays for direct photoreforming of ethanol to hydrogen. Figure 3 shows a comparison of the efficiency of EtOH to H_2 conversion for Au_{np}@TiO_2 nanocavity arrays produced as described above for different Au loadings (experimental details are given in the Supporting Information). Clearly, a loading of 2 nm Au on the TiO_2 cavity leads to the highest H_2 production rate. In Figure 3b, we show that the hydrogen evolution rate is steady over time. Corresponding photocurrent measurements under external bias-free conditions also show a very high stability of the photocurrent magnitude. This indicates that neither significant poisoning of the system nor other deterioration of the catalyst takes place.

The effect of the catalyst geometry is remarkable. In comparison with compact TiO_2 substrates loaded with different amounts of Au and dewetted accordingly, a more than 30-fold increase of the H_2 production efficiency is observed (Figure 3 and SEM images in the Supporting Information). This was tested with different gold loadings at compact layers (Supporting Information, Figure S2b,c), which in both cases resulted in about the same amount at hydrogen generation, that is about 5 μL/9 h. This increase for the cavity embedded Au particles may thus be attributed to the ideal photoreactor conditions described in Figure 1. In control experiments with Au-free TiO_2 (compact or nanocavities), no significant amount of H_2 could be detected under the present conditions. This in line with previous reports, which showed no significant H_2 evolution under open-circuit conditions for co-catalyst-free TiO_2.

In summary, we have introduced an entirely self-organized strategy to create highly defined arrays of metal particles in a cavity. The individual steps used, namely self-organizing anodization and self-ordered dewetting, are both scalable over a large surface area and comparably cheap. Neither self-organization process is limited to the example shown here but may be expanded to a range of self-ordered oxide arrays and dewettable metals.

Therefore, we expect these entirely new structures not only to be a key building block for the creation of highly efficient catalyst/photocatalyst systems but also to have a much wider impact in potentially any application where defined metal/oxide junctions are essential.

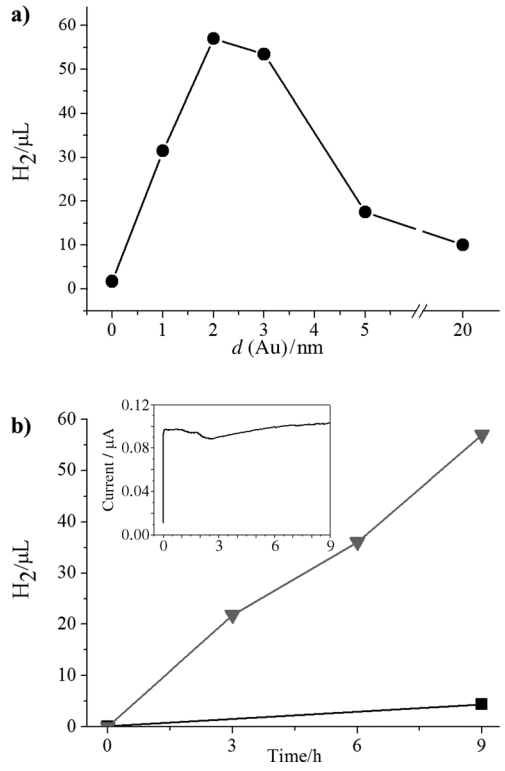

Figure 3. Photocatalytic hydrogen generation with a Au_{np}@TiO_2 nanocavity structure in aqueous EtOH solution. a) H_2 evolution curves, showing the influence of Au layers of different thickness on the TiO_2 nanocavity substrate. b) Influence of UV irradiation time at the Au_{np}@TiO_2 nanocavity (▼) and compact oxide (■) on H_2 generation. Inset: current–time curve of Au_{np}@TiO_2 nanocavities under UV light without applied voltage in aqueous EtOH solution.

Received: March 26, 2013
Published online: June 13, 2013

Keywords: anodization · H_2 production · heterogeneous catalysis · nanocavities · titanium dioxide

[1] I. Paramasivam, H. Jha, N. Liu, P. Schmuki, *Small* **2012**, *8*, 3073.
[2] A. Fujishima, X. Zhang, D. A. Tryk, *Surf. Sci. Rep.* **2008**, *63*, 515.
[3] A. Fujishima, K. Honda, *Nature* **1972**, *238*, 37.
[4] M. R. Hoffmann, S. T. Martin, W. Choi, D. W. Bahnemann, *Chem. Rev.* **1995**, *95*, 69.
[5] A. Linsebigler, G. Lu, J. T. Yates, *Chem. Rev.* **1995**, *95*, 735.
[6] T. L. Thompson, J. T. Yates, *Chem. Rev.* **2006**, *106*, 4428.
[7] G. Palmisano, V. Augugliaro, M. Pagliaro, L. Palmisano, *Chem. Commun.* **2007**, 3425.
[8] D. Ravelli, D. Dondi, M. Fagnonia, A. Albini, *Chem. Soc. Rev.* **2009**, *38*, 1999.
[9] I. Paramasivam, J. M. Macak, P. Schmuki, *Electrochem. Commun.* **2008**, *10*, 71.
[10] X. Quan, S. Yang, X. Ruan, H. Zhao, *Environ. Sci. Technol.* **2005**, *39*, 3770.

[11] Y. Y. Song, F. Schmidt-Stein, S. Berger, P. Schmuki, *Small* **2010**, *6*, 1180.
[12] H. Kato, K. Asakura, A. Kudo, *J. Am. Chem. Soc.* **2003**, *125*, 3082.
[13] T. Kawai, T. Sakata, *Nature* **1980**, *286*, 474.
[14] S. Ono, M. Saito, H. Asoh, *Electrochim. Acta* **2005**, *51*, 827.
[15] K. R. Hebert, S. P. Albu, I. Paramasivam, P. Schmuki, *Nat. Mater.* **2012**, *11*, 162.
[16] S. Hong, T. Kang, D. Choi, Y. Choi, L. P. Lee, *ACS Nano* **2012**, *6*, 5803.
[17] C. V. Thompson, *Annu. Rev. Mater. Res.* **2012**, *42*, 399.
[18] Z. Q. Liu, W. Y. Zhou, L. F. Sun, D. S. Tang, X. P. Zou, Y. B. Li, C. Y. Wang, G. Wang, S. S. Xie, *Chem. Phys. Lett.* **2001**, *341*, 523.
[19] D. Wang, P. Schaaf, *J. Mater. Sci.* **2012**, *47*, 1605.
[20] M. Humenik, Jr., W. D. Kingery, *J. Am. Ceram. Soc.* **1954**, *37*, 18.
[21] A. L. Giermann, C. V. Thompson, *Appl. Phys. Lett.* **2005**, *86*, 121903.

